Effects of Turbulence Parameterization Schemes in Hydrostatic and Nonhydrostatic Shelf Circulation Models

John S. Allen
College of Oceanic and Atmospheric Sciences
Oregon State University
104 Ocean Admin Building
Corvallis, OR 97331-5503
phone: (541) 737-2928 fax: (541) 737-2064 email: jallen@coas.oregonstate.edu

Grant Number: N000140110285

LONG-TERM GOALS

To understand the role of small scale nonhydrostatic processes and turbulent mixing in influencing the mesoscale circulation over the continental shelf.

OBJECTIVES

To evaluate and improve the utilization of turbulence parameterization schemes in hydrostatic and nonhydrostatic shelf circulation models. To apply nonhydrostatic models to studies of relevant three-dimensional coastal flow processes. To determine the requirements for nonhydrostatic model use in coastal flows.

APPROACH

The effects of different parameterization schemes for small scale turbulent mixing are being studied by model-model and model-data comparisons. Both hydrostatic and nonhydrostatic models are being utilized. The motivation for the inclusion of nonhydrostatic Boussinesq models is that nonhydrostatic effects are expected to be an essential component of many important small scale processes involving energetic turbulent mixing over continental shelves. For that purpose, we are initially adapting and applying a nonhydrostatic model developed for study of mesoscale atmospheric processes by Clark (1977). The Clark nonhydrostatic model is finite-difference and is formulated on a C-grid in sigma vertical coordinates. The model has been continuously improved since its origin to include development and testing of two-way nesting available for implementation with multiple nested domains (Clark and Farley, 1984; Clark and Hall, 1991), incorporation of optimal higher order accurate advection schemes (Smolarkiewicz and Clark, 1984) and use of generalized vertical coordinate stretching (Clark and Hall, 1996). The model is well documented (Clark, Hall and Coen, 1996). Recently an MPI (Message Passing Interface) version of the code has been developed to allow for parallel execution on either shared or distributed memory systems. This model has been successfully applied to numerous mesoscale atmospheric problems (e.g., Afanasyev and Peltier (2001a). The Clark model has also recently been used in oceanographic applications by Bush et al., (1995, 1996) to study the formulation of eddies in oceanic jets and by Afanasyev and Peltier (2001b) to study breaking internal waves in Knight Inlet. The hydrostatic model being utilized is ROMS (Shchepetkin and McWilliams, 1998).

Initial applications include experiments relevant to flows over the Oregon continental shelf and slope and focus on model-model comparisons. This research is being carried out jointly with Postdoctoral Research Associate Scott M. Durski. The choice of the Oregon shelf is made to facilitate planned model-data comparisons.

WORK COMPLETED

We have initially considered several shelf flows that can potentially be sensitive to the hydrostatic approximation. These include flow instabilities of the upwelling front and stratified tidally-driven flow over Stonewall Bank. The latter is a prominent small scale topographic feature located on the Oregon continental shelf which is known to cause interesting small scale flow behavior and localized turbulent mixing (Nash and Moum, 2001; Moum and Nash, 2000)

The hydrostatic ROMS model has been used to explore the dynamics of instabilities associated with the coastal upwelling front and the dependence of these instabilities on the turbulence parameterization scheme. An additional objective is to determine the role these instabilities play in across-shelf exchange processes. A number of experiments are run to both gain insight into the processes and understand their potential significance in the real ocean. Simulations are first performed with alongshore-uniform bathymetry and steady upwelling favorable winds applied to an ocean initially at rest to illuminate the development of the instabilities. A sixty-day-record of real wind forcing is then applied over this same domain to examine the response over multiple time-dependent upwelling events. One advantage of this domain is that it allows analysis of alongshore averaged fields for comparison with two-dimensional upwelling simulations which do not exhibit the instabilities. In addition, time-dependent energy exchanges between the alongshore average flow and the perturbations about that average can be analyzed to shed light on the dynamics of the instability. The role of alongshore variations in bathymetry is then considered with both the steady and real wind forcing in a periodic domain with topography representative of the Oregon Shelf.

Studies of tidally-forced flow over small scale topographic features, with characteristics similar to Stonewall Bank, have been initiated using both the nonhydrostatic Clark model and the hydrostatic ROMS model. A separate related study involves the propagation of large amplitude internal waves onshore over continental slope and shelf topography. Initial applications have focused on idealized two-dimensional situations with efforts made to determine the solution dependence on the relevant dimensionless parameters. Extensions to include realistic three-dimensional shelf topography are planned. The nonhydrostatic and hydrostatic solutions are being compared to help understand the limits of validity of the hydrostatic approximation and to learn how the hydrostatic model represents nonhydrostatic processes.

RESULTS

In the study of flow instabilities associated with the upwelling front (Durski and Allen, 2002), we find that with steady winds and alongshore uniform bathymetry instabilities develop on the upwelling front at two separate length scales. Within several days of the onset of upwelling favorable winds a small-scale (8 km) wavelike pattern develops. But as the upwelling progresses a larger scale instability (60 km) forms which eventually dominates the patterns visible in near-surface velocity and density. The two instabilities have different length scales, different rates of development and propagate at different phase speeds along the front. This leads to a complex evolution of the density field with strong meanders and filamentation at the front, despite the simplicity of the domain and forcing. The simulation forced with a time series of real Oregon coast winds shows that although the small scale instabilities dissipate within approximately five days of cessation of upwelling favorable winds, they reappear superimposed on the large scale frontal patterns within several days of each upwelling event. The depth-averaged across-shore velocity field is particularly useful for quantifying the scale and speed of these instabilities in simulations with alongshore uniform bathymetry because it isolates the effects of alongshore variation and thus can be used to quantify differences in the development of these instabilities among sensitivity studies. The left two panels of Figure 1 shows snapshots of the depth averaged across shore velocity field for day 10 of real-wind, uniform-alongshore-bathymetry simulations that differ only in the choice of vertical mixing parameterization. The right two panels show time series of the across-shore averaged alongshore wavenumber spectra for the simulations with the different schemes. The smaller length-scale instabilities dominate the circulation for significantly longer times after model initialization with the Mellor and Yamada (1982) level 2.5 closure (M-Y). In contrast, the simulation with the Large, McWilliams and Doney (1994) K-profile parameterization (KPP) shows the emergence of larger scale patterns within the first 10 days, but still allows for the reappearance of the small scales shortly after the next upwelling favorable wind event occurs on day 13. A perturbation kinetic energy equation can be formulated for this domain by defining velocity and density perturbation fields as deviations from the alongshore averages (Figure 2). Here u and v are the velocity components in the across-shore and alongshore directions respectively. Examination of the terms of the time-averaged perturbation kinetic energy equation (displayed in Figure 2) reveals the dominant role of potential-to-kinetic energy conversion and the significant contribution associated with the across-shore shear in the alongshore velocity field. Simulations with real Oregon coast bathymetry were performed to examine how the growth of these instabilities would be impacted by three-dimensional variations in the background flow field. Figure 3 shows three snapshots of the surface density field for a real-wind, real bathymetry simulation. The offshore position of the upwelling front is found to correlate strongly with the contours of the shelf bathymetery. The instabilities are found to develop and propagate along the front, similar to in the uniform bathymetry case, except where the southern edge of Heceta bank turns sharply shoreward. Here the instabilities appear to 'break' enhancing cross-shore exchange processes.

In Figure 4 we show results from the Clark nonhydrostatic model (CM) and the ROMS hydrostatic model for a two-dimensional numerical experiment with barotropic forcing, at the semi-diurnal tidal frequency, of flow in a stratified coastal ocean over a topographic feature with dimensions similar to Stonewall Bank on the Oregon shelf. In this case, the domain is horizontally periodic with horizontal and vertical dimensions of 30 km and 60 m respectively. The idealized bank has a height of 25 m and a horizontal scale of about 2 km. The maximum barotropic tidal currents away from the bank are 10 cm s^{-1}. The grid resolution is 50 m in the horizontal with 56 vertical sigma levels. The initial density stratification is typical of the Oregon shelf in summer ($N^2 = 2.8 \times 10^{-4}\ s^{-2}$). The generation of internal bore type behavior as the tidally-forced flow goes down the bank is clear. There are appreciable differences in the small scale behavior exhibited in the deformation of the density field in the CM and ROMS solutions with considerably more variability in the nonhydrostatic solution. There are also some interesting differences in the somewhat larger scale behavior in the immediate vicinity of the bores. The dependence of this type of phenomena on the dimensionless parameters of the problem, expressed through variations in dimensional values of tidal current, stratification and bank geometry, is under investigation. Likewise, the solution dependence on the turbulence parameterization scheme is being studied.

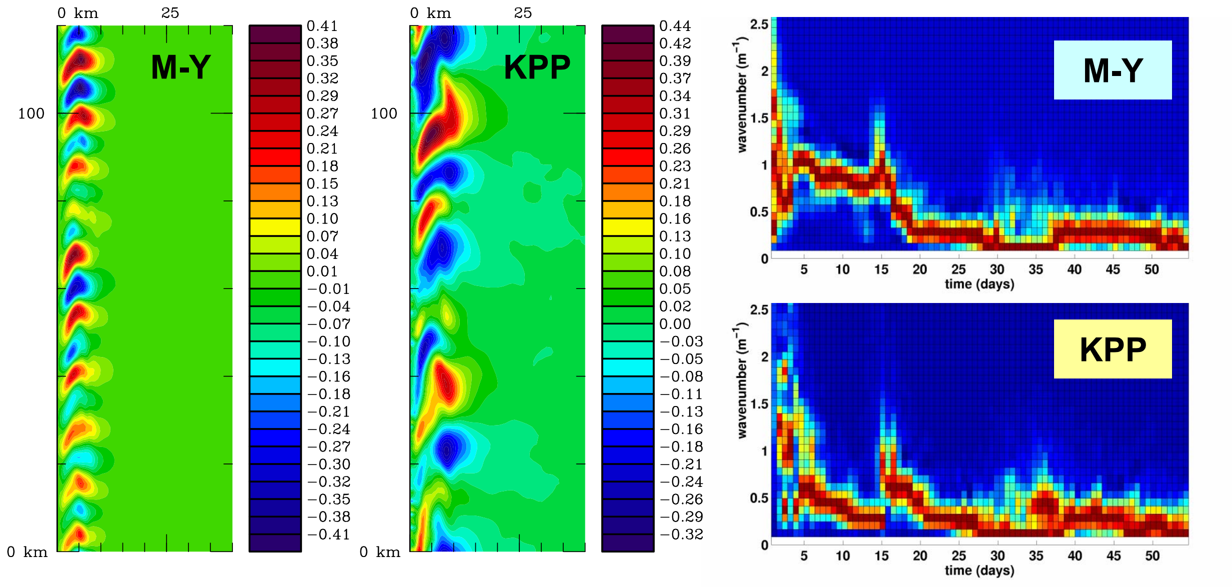

Figure 1. Comparison of simulations using the Mellor-Yamada (M-Y) and the Large, McWilliams and Doney (KPP) parameterizations. Depth-averaged across-shore velocity fields at day 10 show the presence of distinctly different scales of motion with the two schemes. Time series of alongshore power spectra of across-shore velocity show the persistence of small scale instabilities for roughly 10 days longer with the Mellor-Yamada formulation.

$$\frac{\partial\langle KE'\rangle}{\partial t} = -\left\langle \frac{\partial \bar{u}}{\partial x}\overline{u'u'}\rho_0\right\rangle - \left\langle \frac{\partial \bar{v}}{\partial x}\overline{u'v'}\rho_0\right\rangle - \left\langle \frac{\partial \bar{u}}{\partial z}\overline{u'\omega'}\rho_0\right\rangle - \left\langle \frac{\partial \bar{v}}{\partial z}\overline{v'\omega'}\rho_0\right\rangle - g\left\langle \overline{\rho' w'}\right\rangle + dissp.$$

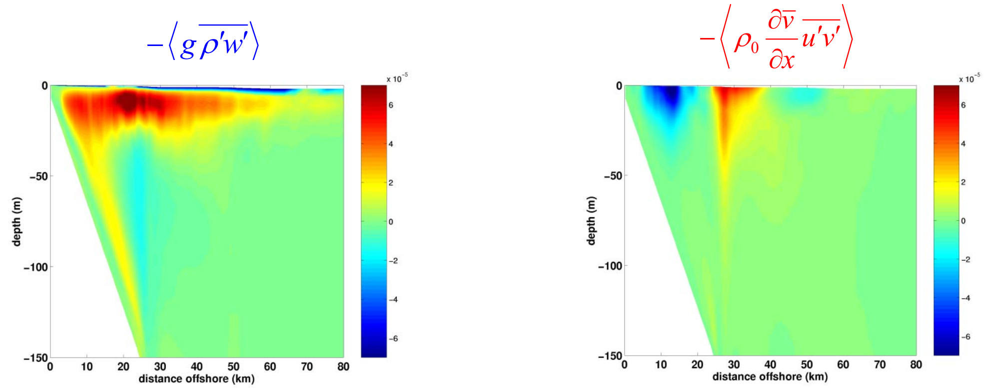

Figure 2. A perturbation kinetic energy equation is formed which describes the energy balance in the deviations about the alongshore averaged state. Overbars indicate alongshore averages and brackets represent time averaging. Examination of the 55-day averaged terms in this equation reveal that the potential-to-kinetic energy conversion term dominates. There is also a significant contribution from across-shore shear of the mean alongshore velocity field. Perturbation kinetic energy is primarily in the upper 30 meters of the water column.

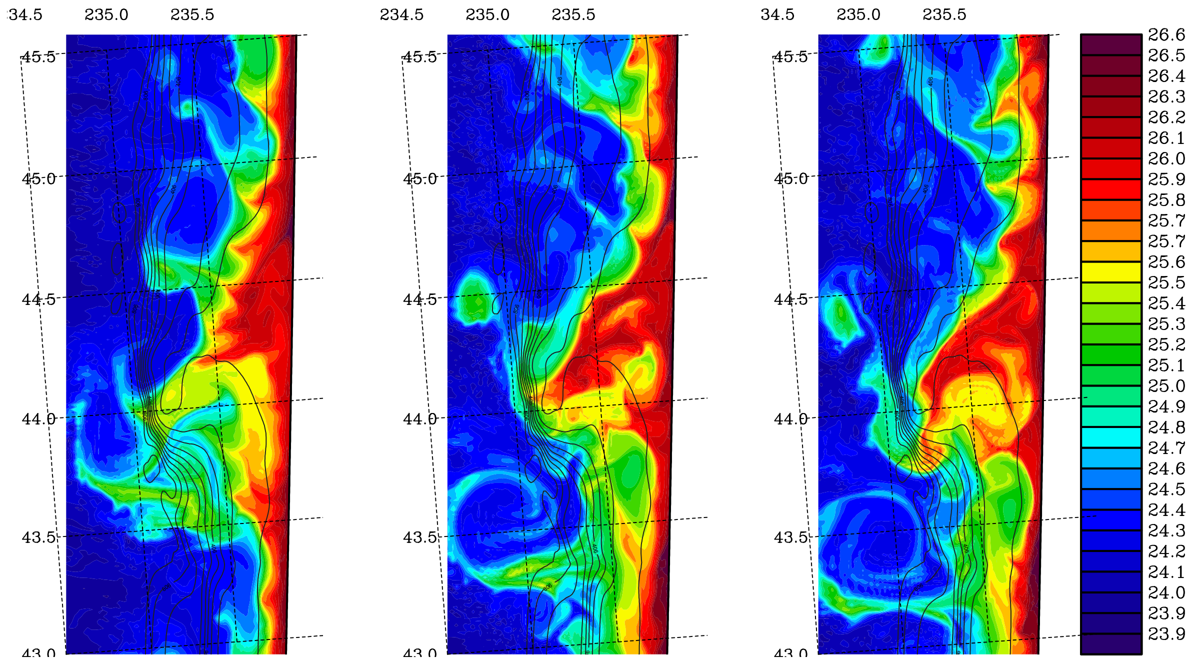

Figure 3. Surface density anomaly fields every two days for a ROMS simulation of wind-driven circulation off the Oregon Coast. Instabilities along the upwelling front propagate offshore following the coastal upwelling jet on the northern side of Heceta bank. 'Breaking' of the instabilities tends to occur where the jet turns sharply shoreward on the southern side of the bank. Propagation of the instabilities can be roughly estimated at between 5 -15 cm/s.

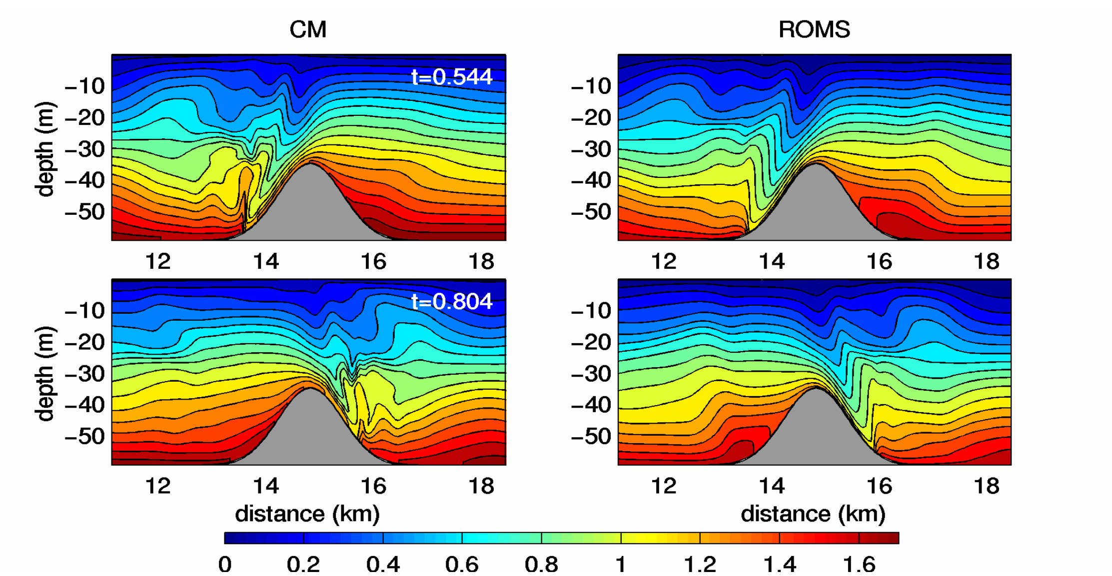

Figure 4. Section plots of potential density anomaly for tidally driven flow over a symmetric bump. Simulations with identical initialization, forcing and resolution were performed with the non-hydrostatic Clark model (left panels) and with the hydrostatic ROMS model (right panel). While the large scale features bear strong resemblance between the models, the non-hydrostatic model solution contains small scale (O(50m)) features in the vicinity of the internal bore which ROMS does not.

REFERENCES

Afanasyev, Ya. D., and W. R. Peltier, 2001a: Numerical simulation of internal wave breaking in the middle atmosphere: The influence of dispersion and three-dimensionalization, *J. of Atm. Sci.*, 58, 132-153.

Afanasyev, Ya. D., and W. R. Peltier, 2001b: On breaking internal waves over the sill in Knight Inlet, Proc. R. Soc. London, Series A., 457, 2799-2825.

Bush, A.B.G., J. C. McWilliams and W. R. Peltier, 1995: The formation of oceanic eddies in symmetric and asymmetric jets. Part I: Early time evolution and bulk eddy transports, *J. Phys. Oceanogr*., 25, 1959-1979.

Bush, A.B.G., J. C. McWilliams and W. R. Peltier, 1996: The formation of oceanic eddies in symmetric and asymmetric jets. Part II: Late time evolution and coherent vortex formation, *J. Phys. Oceanogr.,* 26, 1825-1848.

Clark, T. L., and W. R. Farley, 1984: Severe downslope windstorm calculations in two and three spatial dimensions using anelastic interactive grid nesting: A possible mechanism for gustiness, *J. Atmos. Sci*., 41, 329-350.

Clark, Terry L., and William D. Hall, 1991: Multi-domain simulations of the time dependent Navier Stokes equations: Benchmark error analyses of some nesting procedures, *J. Comp. Phys*., 92, 456-481.

Clark, T. L., and W. D. Hall, 1996: The Design of Smooth, Conservative Vertical Grids for Interactive Grid Nesting with Stretching, *J. Appl. Meteor*., 35, 1040-1046.

Clark, T. L., W. D. Hall and J. L. Coen, 1996: Source code documentation of the Clark-Hall cloud-scale model. NCAR Tech Note NCAR/TN-426+STR.

Durski, S. M. and J. S. Allen, 2002: A modeling study of the flow instability associated with the coastal upwelling front, Abstract. 2002 Ocean Sciences Meeting, EOS, 83:4, pOS 375.

Large, W. G., J. C. McWilliams, and S. D. Doney, 1994: Oceanic vertical mixing: A review and a model with a nonlocal boundary layer parameterization, *Rev. Geophys*., 32, 363-403.

Mellor, G. L., and T. Yamada, 1982: Development of turbulence closure model for geophysical fluid problems, *Rev. Geophysics Space Phys*., 10, 851-875.

Moum, J. N., and J. D. Nash, 2000: Topographically-induced drag and mixing at a small bank on the continental shelf, *J. Phys. Oceanogr*, 30:2049-2054.

Nash, J. D., and J. N. Moum, 2000: Internal hydraulic flows on the continental shelf: high drag states over a small bank, *J. Geophys. Res*., 106:4593-4611.

Shchepetkin, A. F., and J. C. McWilliams 1998: Quasi-monotone advection schemes based on explicit locally adaptive dissipation, *Monthly Weather Rev*., 126, 1541-1580.